Pflugers Arch - Eur J Physiol (2017) 469:1313–1323
DOI 10.1007/s00424-017-1998-7

Transient receptor potential vanilloid 4 (TRPV4) channel as a target of crotamiton and its bimodal effects

Hiroki Kittaka[1] · **Yu Yamanoi**[1,2,3] · **Makoto Tominaga**[1,2,4]

Received: 21 January 2017 / Revised: 2 May 2017 / Accepted: 12 May 2017 / Published online: 13 June 2017

Abstract The sensation of itching can be defined as "an unpleasant cutaneous sensation that provokes a desire to scratch." The perception of itching is not critical for the maintenance of life, but persistent itching can be extremely irritating and decreases the quality of life. Crotamiton (*N*-ethyl-*o*-crotonotoluidide) has been used as an anti-itch agent for humans for around 70 years. In spite of the long use of crotamiton, its mechanism of action remains unknown. We hypothesized that crotamiton might have effects on transient receptor potential (TRP) channels expressed in the peripheral nervous system and the skin. We first examined the effects of crotamiton on TRP channels by whole-cell patch-clamp recordings. We found that crotamiton strongly inhibited TRPV (vanilloid) 4 channels followed by large currents after crotamiton washout. In mice, crotamiton inhibited itch-related behaviors induced by a TRPV4-selective agonist (GSK1016790A). We biophysically investigated the large TRPV4 currents after crotamiton washout. Comparing single-channel open probabilities and current amplitudes of TRPV4, increases in both parameters were found to contribute to the large washout currents of TRPV4. Because the change in current amplitudes suggested pore dilation of TRPV4, we examined this possibility with cation replacement experiments and by measuring changes in reversal potentials. Greater cation influxes and changes in reversal potentials upon crotamiton washout were observed, suggesting that the TRPV4 pore dilated in its uninhibited state. From these results, we identified the molecular target of crotamiton as TRPV4 and demonstrated pore dilation of TRPV4 upon crotamiton washout.

Keywords Crotamiton · TRPV4 · Pore dilation · Itch

Hiroki Kittaka and Yu Yamanoi contributed equally to this work.

Electronic supplementary material The online version of this article (doi:10.1007/s00424-017-1998-7) contains supplementary material, which is available to authorized users.

✉ Makoto Tominaga
tominaga@nips.ac.jp

[1] Division of Cell Signaling, Okazaki Institute for Integrative Bioscience (National Institute for Physiological Sciences), National Institutes of Natural Sciences, 5-1 Higashiyama, Myodaiji, Okazaki, Aichi 444-8787, Japan

[2] Department of Physiological Sciences, The Graduate University for Advanced Studies (SOKENDAI), 5-1 Higashiyama, Myodaiji, Okazaki, Aichi 444-8787, Japan

[3] Research Laboratory, Ikedamohando Co., Ltd., 16 Jinden, Kamiichi, Nakaniikawa, Toyama 930-0394, Japan

[4] Institute for Environmental and Gender-Specific Medicine, Juntendo University, Chiba 279-0021, Japan

Introduction

Itching is an unpleasant cutaneous sensation that provokes a desire to scratch the surface of the skin [41]. Acute itching is caused by allergens, mosquito bites, and some chemical compounds [26]. Chronic itching is a frequent consequence of atopic dermatitis, kidney failure, cholestasis, and neuronal lesions [19]. To relieve the sensation of itching with medication, antihistamines such as diphenhydramine, steroids such as dexamethasone, local anesthetics such as lidocaine, and a kappa opioid receptor agonist, nalfurafine, have been used. Crotamiton (*N*-ethyl-*o*-crotonotoluidide) is not categorized into any of those antipruritics. Rather, 10% crotamiton ointment was initially reported as a scabicide in clinical trials with a cure rate of 95–96% [2, 27]. Scabies is caused by skin infestation by mites such as *Sarcoptes scabiei*. Although crotamiton was initially screened as a synthetic parasiticidal

chemical [13], it was also clinically tested for relief from itching [12]. For the treatment of scabies, crotamiton is applied to the entire body for two successive nights and no cutaneous irritation was observed [13]. Therefore, crotamiton was found to be biologically safe and it was clinically proven to be effective for the relief of itching [12]. However, its molecular mechanisms remain to be elucidated.

Transient receptor potential (TRP) channels constitute an ion channel superfamily having non-selective cation permeability [50]. TRP channels were first characterized in a fruit fly with a mutation showing an abnormal photoresponsiveness [33]. In mammals, TRP channels are comprised of six related protein families consisting of TRPA (ankyrin), TRPC (canonical), TRPM (melastatin), TRPML (mucolipin), TRPP (polycystin), and TRPV (vanilloid) [50]. TRP channels are best recognized for their contribution to sensory transduction, including temperature, pain, itch, touch, osmolarity, pheromones, and various other stimuli originating from both within and outside of the cell [50]. Among TRP channels, TRPA1, TRPM2, TRPM3, TRPM8, TRPV1, TRPV2, and TRPV4 channels are expressed in sensory neurons such as dorsal root ganglion (DRG) neurons and trigeminal ganglion neurons [4, 5, 15, 32, 37, 39, 44, 53] that peripherally sense external stimuli as mentioned above. On the other hand, TRPV3 and TRPV4 are mainly expressed in skin keratinocytes [9, 16, 40, 43, 59]. Interestingly, all of these TRP channels are activated or modulated by temperature; thus, they are also called thermosensitive TRP channels [4, 5, 9, 15, 16, 32, 39, 40, 43, 44, 48, 53, 59]. Some of these TRP channels are reportedly involved in itching sensation as stated below [26].

With regard to the mechanisms of action of crotamiton, it does not possess antihistaminergic, anti-inflammatory, or local anesthetic effects and it does not have a steroidal structure. Therefore, we hypothesized that the molecular targets for crotamiton are TRP channels that are expressed in peripheral neurons and skin keratinocytes. We screened the ability of crotamiton to affect TRPA1 [44], TRPM8 [32, 39], TRPV 1 [4], TRPV2 [5], TRPV3 [9, 40, 43, 59], and TRPV4 [15, 16] channels, most of which were reported to be involved in itching sensations. For example, TRPV1 transmits histaminergic itching sensations via phospholipase A_2(PLA_2)/lipoxygenase or $G_{q/11}$/PLCβ3 signaling [17, 20, 24, 42]. TRPA1 is involved in non-histaminergic itching induced by chloroquine [57], bovine adrenal medulla 8–22 [57], thymic stromal lymphopoietin [58], and serotonin [34]. Gain of function point mutations of TRPV3 such as Gly573Ser, Gly573Cys, and Trp692Gly, which are involved in Olmsted syndrome, are associated with itching [31]. TRPV4 is involved in serotoninergic itch [1], histaminergic itch [7], and TRPV1-dependent itch [25]. We, therefore, focused on the molecular mechanisms of crotamiton, and we investigated the modulatory effects of crotamiton on the above six TRP channels using a patch-clamp technique with whole-cell and single-channel configurations.

Results

Crotamiton inhibited GSK-activated TRPV4 currents and reduced GSK-induced itch-related behaviors

We conducted whole-cell patch-clamp recordings with HEK293T cells that expressed each of the above TRP channels (mTRPA1, mTRPM8, mTRPV1, mTRPV2, mTRPV3, and mTRPV4). Crotamiton did not activate any of these channels (Supplementary Fig. 1). In addition, crotamiton and TRP ligands did not activate membrane currents in the mock-transfected cells (Supplementary Fig. 3a). However, crotamiton did inhibit mTRPA1, mTRPM8, mTRPV2, and mTRPV4 when the extracellular medium was calcium-free (Table 1 and Supplementary Fig. 1). Crotamiton strongly inhibited mTRPV4 currents with the lowest IC_{50} value among these TRP channels under more physiological condition with 2 mM extracellular calcium (Table 1 and Supplementary Fig. 2). Therefore, we focused on mTRPV4 in the following investigation.

mTRPV4 currents activated by the TRPV4-selective agonist GSK1016790A (GSK) [46, 47] were inhibited by crotamiton in a dose-dependent manner in 2 mM extracellular calcium (Figs. 1a and 2a) and extracellular calcium-free conditions (Figs. 1b and 2b). Surprisingly, rapidly activating and larger mTRPV4 currents than those induced by GSK alone were observed upon crotamiton washout when the extracellular medium was calcium-free (Fig. 1b). When crotamiton was applied with GSK, crotamiton did not completely inhibit GSK-activated mTRPV4 currents even at higher concentrations (Fig. 1c). However, clear and large washout currents were observed (Fig. 1c). The results suggested that removal of crotamiton resulted in rapid reactivation of mTRPV4 activated by GSK. The washout currents were only observed during co-application of GSK and crotamiton, and not with GSK alone (Fig. 1d) or crotamiton alone (Supplementary Fig. 3b). These phenomena were also observed in normal human epidermal keratinocytes (NHEK) (Fig. 1e), suggesting that a similar mechanism is working in native cells, although we do not know which TRPV4, that in neurons or in keratinocytes, shows these phenomena. In order to examine the voltage dependency of the crotamiton effects, we analyzed GSK-induced mTRPV4 currents with or without crotamiton by applying voltage-ramp pulses from −100 to +100 mV and constructed current–voltage (*I–V*) curves. GSK induced outwardly rectifying mTRPV4 currents that were inhibited by crotamiton in a dose-dependent manner in the presence of 2 mM

Table 1 IC_{50} values of TRP channels inhibited by crotamiton

IC_{50} (μM)	mTRPA1	mTRPM8	mTRPV1	mTRPV2	mTRPV3	mTRPV4
0 mM Ca^{2+}	296.6	283.0	NE	97.5[a]	NE	223.5
2 mM Ca^{2+}	>500	268.2	–	>500	–	15.5

NE no effect

[a] IC_{50} value was obtained with a dose–response curve for crotamiton up to 1 mM

extracellular calcium (Fig. 2a and Supplementary Fig. 2). Crotamiton-induced, dose-dependent inhibition of GSK-activated mTRPV4 currents was also observed in extracellular calcium-free medium. The *I–V* relationship of the

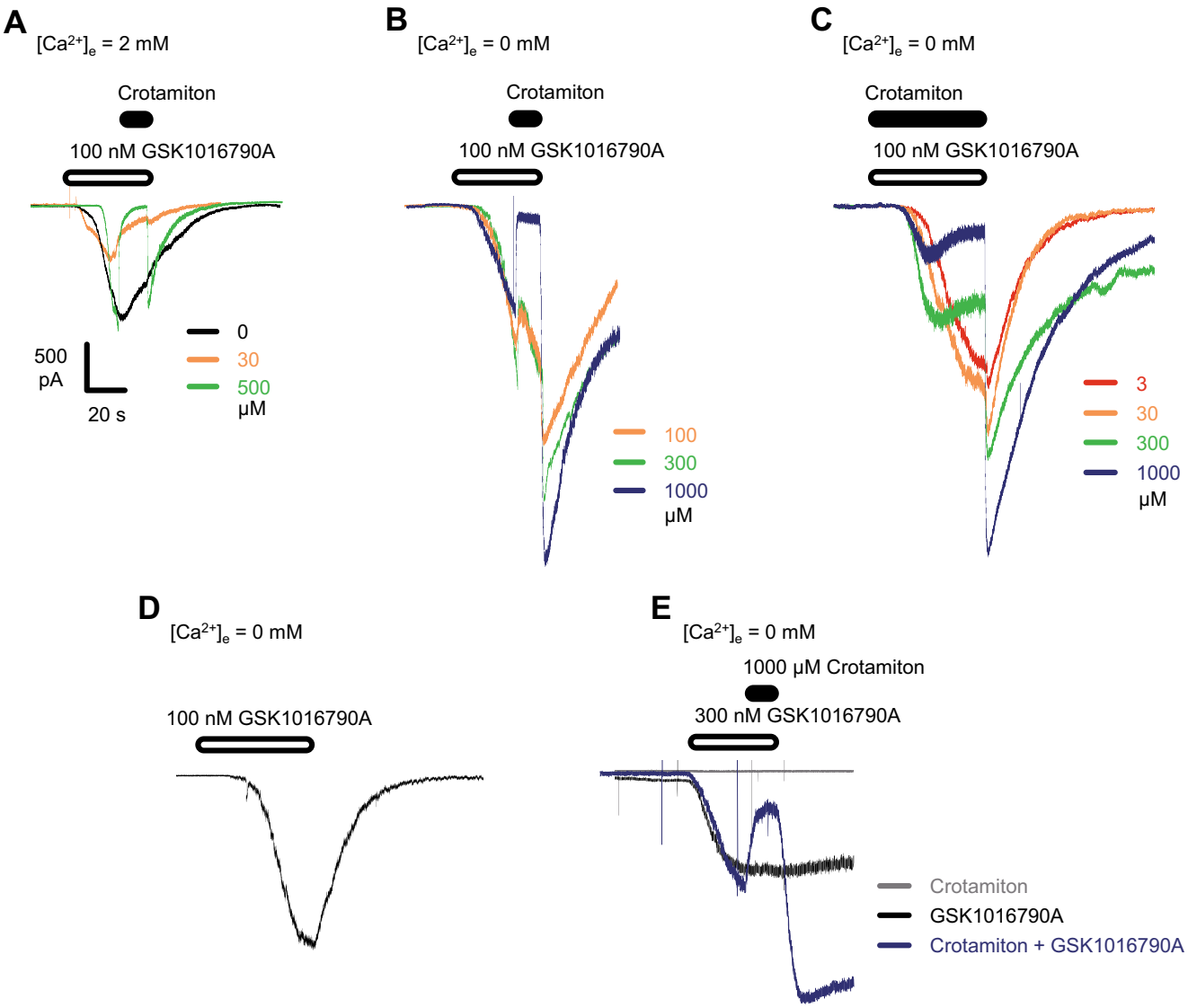

Fig. 1 Characterization of TRPV4 inhibition and activation upon crotamiton treatment in whole-cell recordings. **a** Superimposed representative traces of mTRPV4 inward currents at −60 mV in 2 mM extracellular calcium. One hundred nanomolars of GSK1016790A (GSK)-induced mTRPV4 inward currents was inhibited by crotamiton (500 μM). $n = 11$, 5, and 5 for 0, 30, and 500 μM crotamiton, respectively. **b** Superimposed representative traces of mTRPV4 inward currents in the absence of extracellular calcium. GSK-induced mTRPV4 inward currents were inhibited by crotamiton in a dose-dependent manner, followed by larger currents upon washout of GSK with crotamiton than GSK-induced currents. $n = 6$, 6, and 8 for 100, 300, and 1000 μM crotamiton, respectively. **c** Superimposed representative traces of mTRPV4 inward currents upon simultaneous application of GSK and crotamiton in the absence of extracellular calcium. $n = 4$, 5, 5, and 5 for 3, 30, 300, and 1000 μM crotamiton, respectively. **d** A representative trace of mTRPV4 inward currents upon GSK application in the absence of extracellular calcium. $n = 7$. **e** Superimposed representative traces of GSK-induced currents in normal human epidermal keratinocytes in the absence of extracellular calcium

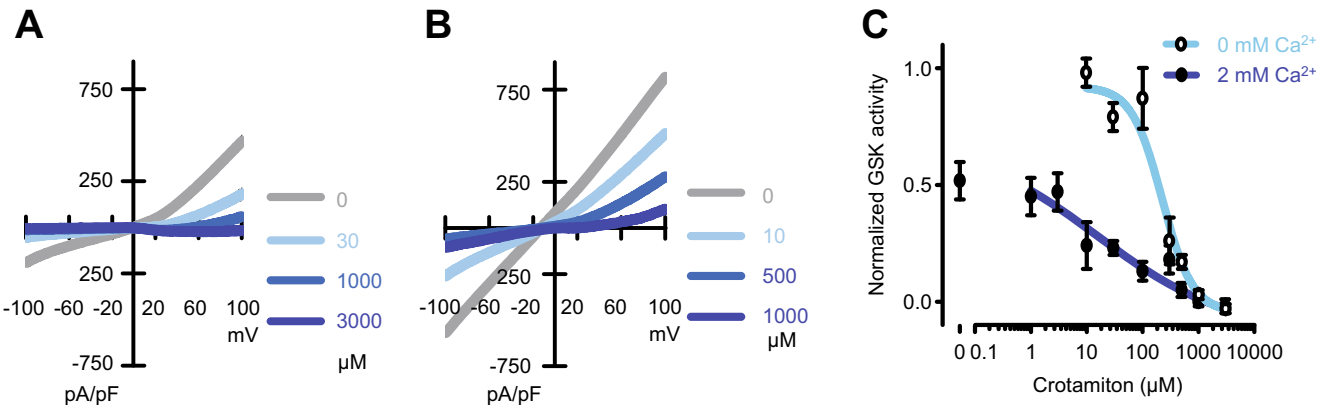

Fig. 2 *I–V* relationships of mTRPV4 inhibition upon crotamiton treatment in whole-cell recordings. **a**, **b** Current–voltage (*I–V*) relationships of mTRPV4 currents inhibited by crotamiton in 2 mM calcium (**a**) and in the absence of extracellular calcium (**b**) in different crotamiton concentrations. Means ± SEM. n = 25, 8, 10, and 7 for 0, 30, 1000, and 3000 μM crotamiton, respectively (**a**). n = 33, 11, 8, and 7 for 0, 10, 500, and 1000 μM crotamiton, respectively (**b**). **c** Dose-dependent inhibition curves of mTRPV4 inward currents at −60 mV by crotamiton in 2 mM extracellular calcium (*black circle*) and extracellular calcium-free (*white circle*) conditions. Means ± SEM. n = 11, 6, 7, 6, 6, 6, 7, 5, 6, and 5 for 0, 1, 3, 10, 30, 100, 300, 500, 1000, and 3000 μM crotamiton, respectively (*black circle*). n = 4, 7, 6, 6, 3, 8, and 8 for 10, 30, 100, 300, 500, 1000, and 3000 μM crotamiton, respectively (*white circle*)

mTRPV4 currents without calcium was linear as reported [30, 45, 52, 54] (Fig. 2b). These data suggested that crotamiton-induced inhibition of mTRPV4 currents was voltage-independent regardless of extracellular calcium. Figure 2c shows dose–response curves of crotamiton-induced inhibition of mTRPV4 activated by GSK in the presence and absence of extracellular calcium. IC_{50} values for mouse and human TRPV4 were 15.5 and 16.3 μM, respectively, in the presence of 2 mM extracellular calcium, whereas it was 223.5 μM for mTRPV4 in the absence of extracellular calcium (Table 1 and Fig. 2c). In the presence of extracellular calcium, the activity was lower than in the absence of calcium because extracellular calcium reduced the current amplitude of TRPV4 [45, 54]. Furthermore, crotamiton significantly reduced the GSK-induced itch-related behaviors in mice (Fig. 3). Taken together, crotamiton is an inhibitor of TRPV4 channels, and the antipruritic effect of crotamiton is due, to some extent, to the inhibition of TRPV4.

Crotamiton induced large washout currents after GSK-induced mTRPV4 activation

In order to examine the mechanism of crotamiton action in the washout, we conducted single-channel recordings using inside-out excised membrane patches of HEK293T cells expressing mTRPV4. GSK (10 nM) induced a single-channel activity of mTRPV4 (unitary amplitude = 2.0 ± 0.4 pA, NP_o = 0.7 ± 0.1, n = 11). The resulting single-channel conductance (32.8 ± 5.8 pS) was similar to the reported values ranging from 30.4 to 61.4 pS [45, 55]. The GSK-induced single-channel currents were inhibited by crotamiton (1000 μM) (unitary amplitude = 1.6 ± 0.3 pA, NP_o = 0.2 ± 0.1, n = 11), and large washout currents with large unitary amplitudes were observed (unitary amplitude = 4.1 ± 1.0 pA, NP_o = 0.8 ± 0.1, n = 11) (Fig. 4a, b), which was consistent with the results obtained in the whole-cell recordings (Fig. 1b). NP_o values of the GSK-induced single-channel currents were significantly decreased

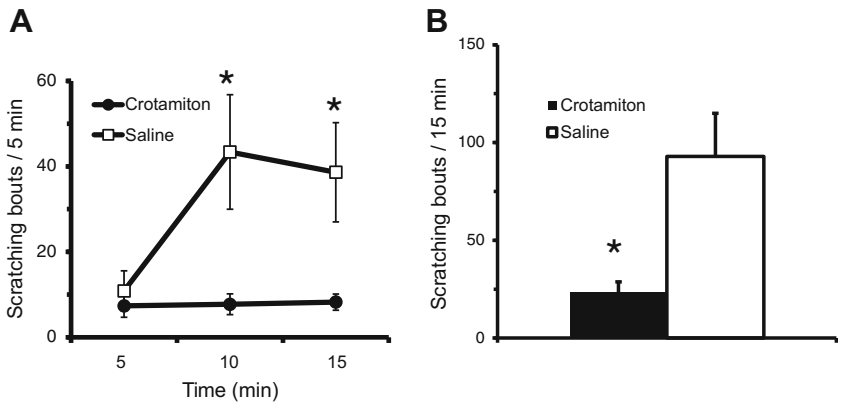

Fig. 3 GSK1016790A-induced itch-related behaviors upon crotamiton treatment of mice. **a**, **b** Scratching behaviors induced by injection of GSK (10 nmol/50 μL per site) into the back skin of mice were assessed every 5 min (**a**) or for total of 15 min (**b**). Means ± SEM. n = 8. *p < 0.05

by crotamiton. Both unitary amplitudes and NP_o values became significantly larger upon its washout. Consistent with the results obtained in the whole-cell recordings (Fig. 1c), some single-channel currents were observed in the simultaneous application of GSK and crotamiton (unitary amplitude = 1.7 ± 0.3 pA, NP_o = 0.3 ± 0.1, n = 13). Both unitary amplitudes and NP_o values became significantly larger upon washout (unitary amplitude = 3.4 ± 0.5 pA, NP_o = 0.7 ± 0.3, the, n = 14) (Fig. 4c, d). These data suggested that crotamiton changed ion permeation.

Crotamiton induced mTRPV4 pore dilation

Next, we examined whether mTRPV4 permeability was increased upon crotamiton washout at a macroscopic current level, which was suggested in the single-channel analysis (Fig. 4). We substituted all the extracellular sodium ions with organic methylamine or tetramethylammonium ions to estimate the pore sizes of the mTRPV4 channels in a non-dilated state [8, 22]. Substituted cations were as follows: mono methylamine [MMA, CH_3NH_2, diameter (α) = 2.00 Å], dimethylamine [DMA, $(CH_3)_2NH$, α = 4.20 Å], tetramethylammonium ion [$TetMA^+$, $(CH_3)_4N^+$, α = 6.48 Å], and *N*-methyl-D-glucamine (NMDG, α = 8.90 Å) [8]. Whole-cell patch-clamp recordings using HEK293T cells expressing mTRPV4 were performed. After mTRPV4 activation by GSK, cation-substituted solutions with GSK were applied (Fig. 5a). mTRPV4 currents by MMA, DMA, $TetMA^+$, and NMDG were 1.55 ± 0.49 (n = 3), 0.32 ± 0.15 (n = 6), 0.05 ± 0.02 (n = 4), and 0.03 ± 0.01 (n = 9), respectively (Fig. 5a, c). NMDG completely inhibited mTRPV4 currents induced by GSK and very small mTRPV4 currents were observed in the $TetMA^+$ solution. On the other hand, mTRPV4 currents were not inhibited in the MMA or DMA solutions, indicating that the pore diameter of mTRPV4 activated by GSK was between 4.20 and 6.48 Å. In addition, the mTRPV4 currents become even larger in the MMA and DMA solutions (Fig. 5a, c), indicating that MMA and DMA were more permeable than sodium ions. Similarly, by using cation-substituted solutions, mTRPV4 currents caused by crotamiton washout were recorded in HEK293T cells expressing mTRPV4. GSK and crotamiton were co-applied for 60 s in cation-substituted conditions as shown in Fig. 5b and the washout currents of mTRPV4 were measured. In the solutions of MMA, DMA, and $TetMA^+$, significant mTRPV4 currents were observed (MMA = 1.07 ± 0.19 nA, n = 5; DMA = 0.90 ± 0.29 nA, n = 4; $TetMA^+$ = 0.22 ± 0.07 nA, n = 10) (Fig. 5b, c). Those results indicated that in addition to MMA and DMA (Fig. 5a, c), $TetMA^+$ permeated through the mTRPV4 channel pore (note the comparison of TRPV4-mediated current sizes (Fig. 5c)). When the extracellular cation was substituted with NMDG, no measurable currents were observed (n = 4) (Fig. 5b), suggesting that the pore diameter of mTRPV4 after washout of crotamiton with GSK was between 6.48 and 8.90 Å.

The permeation of larger cations through the mTRPV4 pore upon washout of crotamiton with GSK indicated pore dilation. Therefore, in order to confirm the permeability changes of mTRPV4 upon crotamiton washout shown in Fig. 5b, the changes in reversal potentials were examined. The extracellular cations were substituted with $TetMA^+$ and the intracellular solution was a sodium-based normal bath solution (see "Experimental procedures") [6, 23, 46, 51]. Voltage ramps from −90 to 0 mV were delivered every 2 s with a holding potential of −60 mV. After co-application of crotamiton and GSK for 60 s, the reversal potential shifted from −41.2 to −23.4 mV in 110 s (Fig. 6a), indicating that $TetMA^+$ permeated the mTRPV4 pore upon washout of crotamiton with GSK although $TetMA^+$ almost completely inhibited GSK-induced mTRPV4 currents (Fig. 5a, c). The rate of reversal potential shift +4.85 mV/0.5 min in the cell shown in Fig. 6a is similar to that observed in the ATP-gated cation channel P2X4 (+4.42/0.5 min) [23]. Pore dilation was previously reported not only in ATP-gated channels such as P2X2 [23, 46], P2X4 [23, 46], and P2X7 [23, 51] but also in TRPA1 [6, 22], TRPV1 [11, 35], and TRPV3 [10] channels, supporting the idea that some TRP channels share this property. Mean reversal potential shift (8.27 ± 1.31 mV, n = 11) was statistically significant (Fig. 6b).

Discussion

Crotamiton ointment has been used for itch relief for a very long time [12], although the mechanisms of action have been unclear. Therefore, we hypothesized that the molecular target of crotamiton is a molecule involved in itch sensation and expressed in the peripheral neurons or the skin keratinocytes. Thus, we examined TRPA1 [44], TRPM8 [32, 39], TRPV1 [4], TRPV2 [5], TRPV3 [40, 43, 59], and TRPV4 [9, 16]]. We eventually identified TRPV4 as the target. TRPV4 is expressed in DRG neurons [15] and skin keratinocytes [9, 16]. Because TRP channel functions are regulated by calcium ions [21, 32, 36, 49, 54, 59], whole-cell patch-clamp recordings were performed in the absence of extracellular calcium or in 2 mM extracellular calcium. Crotamiton did not activate any of the six TRP channels examined and inhibited TRPA1, TRPM8, TRPV2, and TRPV4 channels to different extents (Supplementary Fig. 1). In the presence of 2 mM extracellular calcium, TRPV4 was found to have the lowest IC_{50} value for crotamiton-induced inhibition among the four TRP channels (Table 1). TRPV4 is a member of the TRP channel superfamily activated by hypotonic stimulation [30], warm temperature [9, 14, 16], arachidonic acid metabolite 5′, 6′-epoxyeicosatrienoic acid [56], and synthetic ligands such as

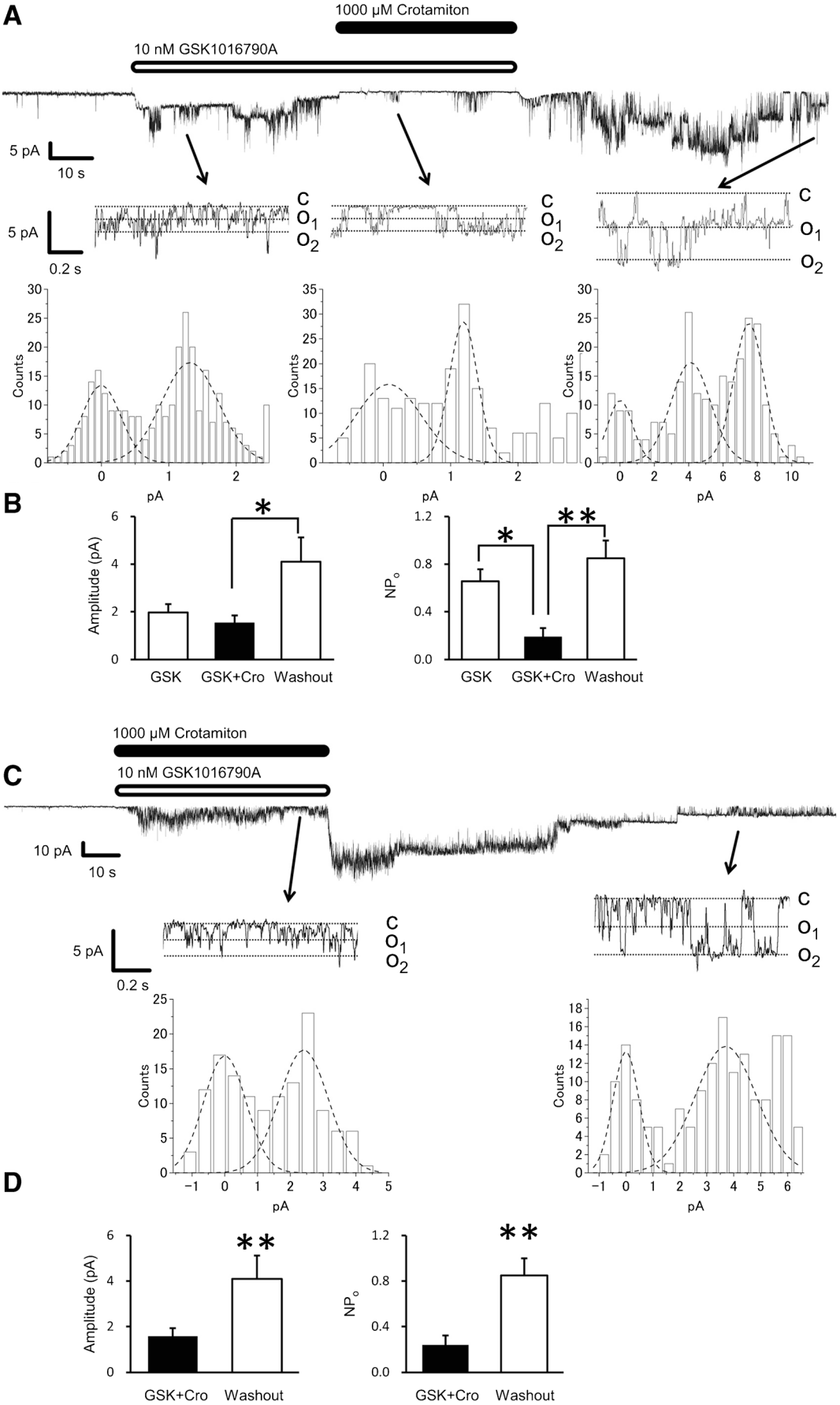
A
1000 μM Crotamiton
10 nM GSK1016790A
5 pA
10 s
5 pA
0.2 s
C
O1
O2
Counts
pA
B
Amplitude (pA)
NPo
GSK
GSK+Cro
Washout
C
1000 μM Crotamiton
10 nM GSK1016790A
10 pA
10 s
5 pA
0.2 s
D

◀ **Fig. 4** Single-channel currents of mTRPV4 channels upon crotamiton treatment. **a** A representative trace of mTRPV4 currents, magnified traces, and histograms indicated by *arrows*. *C* close. *O* open. Membrane potential was held at −60 mV. **b** Averaged values of unitary amplitudes and NP_o (channel number × open probability) for the currents with GSK treatment alone (*GSK*), GSK with crotamiton (*GSK+Cro*), and crotamiton washout (*Washout*). Means ± SEM. n = 10, 11, and 11 for GSK, GSK+Cro, and Washout, respectively. *$p < 0.05$. **c** A representative trace of mTRPV4 single-channel currents, magnified traces, and histograms indicated by *arrows*. *C* close. *O* open. Membrane potential was held at −60 mV. **d** Averaged values of unitary amplitudes and NP_o for the currents with GSK with crotamiton (*GSK+Cro*) and crotamiton washout (*Washout*). Means ± SEM. n = 13, 14. *$p < 0.05$

4 alpha-phorbol 12,13-didecanoate [54] and GSK1016970A [47]. TRPV4 was reported to be involved in itch caused by serotonin [32] and histamine [33] and itch depending on TRPV1 [34]. Therefore, we examined the effects of crotamiton on GSK1016970A-induced itch-related behaviors in vivo. We found that crotamiton significantly reduced the GSK1016790A-induced scratching behaviors (Fig. 3), suggesting that the antipruritic effect of crotamiton is due to the inhibition of TRPV4 to some extent.

Indeed, crotamiton rapidly inhibited GSK-activated mTRPV4 currents in HEK293T cells at both whole-cell and single-channel levels (Figs. 1, 2, and 4). However, the unitary amplitudes of TRPV4 currents were not changed with crotamiton. This result suggests that the effects of crotamiton are due to inhibition of the frequency of channel opening and not the blocking of permeation. Surprisingly, mTRPV4 currents became even larger after crotamiton washout. To estimate the possibility of pore dilation of mTRPV4, we performed current recordings (Fig. 5) and reversal potential shift experiments using large diameter cations (Fig. 6). Although the significance of the shift of reversal potentials as a marker for pore dilation is under debate [28], these data support the notion of pore dilation. Therefore, the washout currents could be explained by pore dilation of mTRPV4 activated by GSK. The physiological functions of pore dilation of TRPV4 in vivo are still unclear because sudden removal of crotamiton from the skin would be difficult. Clarification of the sites of action of crotamiton would be intriguing.

In a phylogenetic tree of the TRPV subfamily, TRPV4 is located between TRPV1 and TRPV3 [59], both of which have shown pore dilation [10, 11, 35], suggesting that TRPV1, TRPV3, and TRPV4 acquired the property during evolution. Together with the fact that TRPA1 shares the same property [6, 22], pore dilation could be a common property of a subset

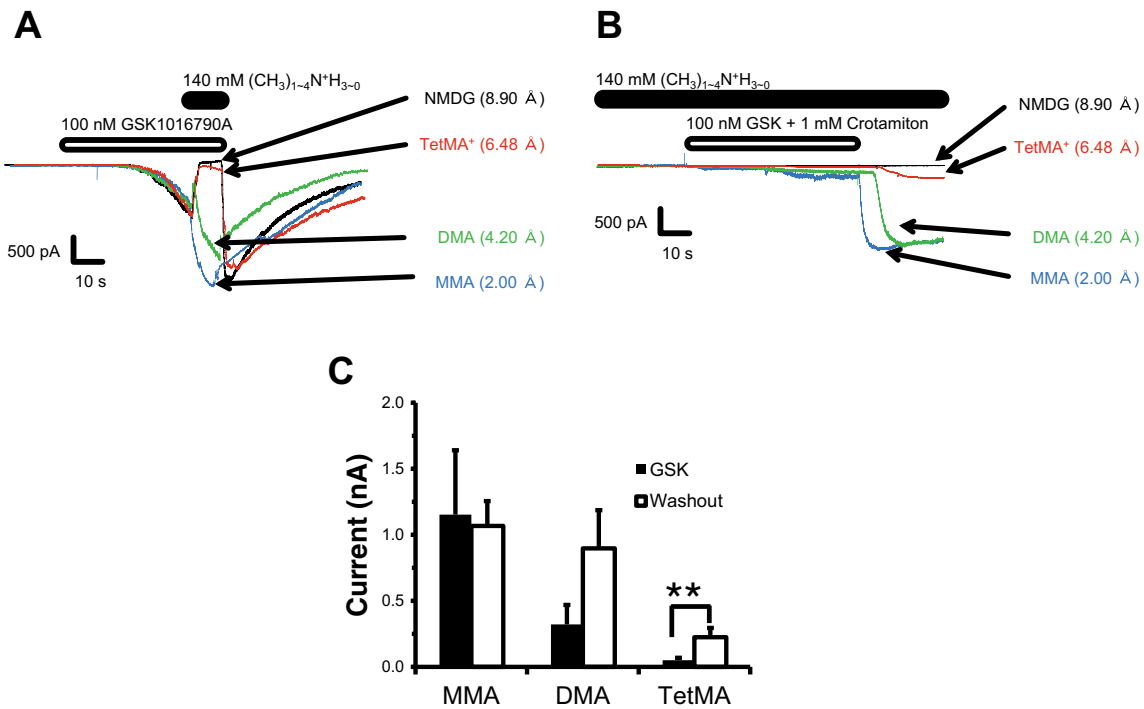

Fig. 5 Pore dilation of mTRPV4 upon crotamiton washout. **a** Superimposed representative traces of mTRPV4 inward currents activated by GSK in the indicated cation solutions with predicted pore sizes in the parenthesis. GSK-induced inward currents of mTRPV4 were inhibited by tetramethylammonium ions (*TetMA*) and *N*-methyl-D-glucamine (*NMDG*). *MMA* monomethylamine, *DMA* dimethylamine. Holding potential was −60 mV. **b** Superimposed representative traces of mTRPV4 inward currents treated with GSK and crotamiton in the indicated cation solutions. Holding potential was −60 mV. **c** Averaged mTRPV4 current sizes without crotamiton (*GSK*) or crotamiton washout (*Washout*) in the indicated cation solutions. Holding potential was −60 mV. Means ± SEM. n = 3, 6, and 4 (without crotamiton) and 5, 4, and 10 (washout). *$p < 0.05$

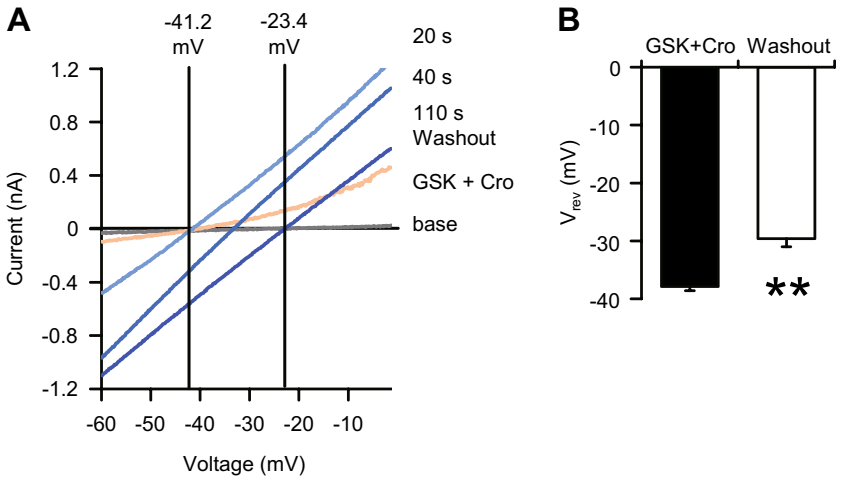

Fig. 6 Shift of reversal potentials for mTRPV4 currents upon crotamiton washout. **a** Representative current–voltage curves of mTRPV4 whole-cell currents with Na^+ (inside) and $TetMA^+$ (outside) solutions upon washout of GSK and crotamiton (GSK+Cro and Washout, respectively) with time. Holding potential was −60 mV. Voltage-ramp pulses from −90 to 0 mV in 500 ms were delivered every 2 s. **b** Changes in reversal potential (V_{rev}) of mTRPV4 currents with GSK and crotamiton (*GSK+Cro*) and their washout (110 s, *Washout*). $N = 11$. $^{**}p < 0.01$

of TRP channels expressed in sensory neurons and skin keratinocytes, and the similarities could provide clues to its physiological significance. The structure of three (TRPA1 [38], TRPV1 [3, 29], and TRPV2 [18, 60]) of the six TRP channels examined in this study were analyzed at the atomic level. Ion permeation pathways in the natural agonist-bound form were clarified for TRPA1 [38] and TRPV1 [3]. The widest central cavity of the ion permeation pathway of aryl isothiocyanate (AITC)-bound TRPA1 is about 4.5 Å [38], and that of capsaicin-bound TRPV1 is about 4.6 Å [3], both of which are close to the pore size of TRPV4 estimated by permeant ions in this study (4.20–6.48 Å). Although the dilated pore sizes differ between TRPA1/TRPV1 and TRPV4 based on the NMDG permeability, future comparisons of the channel structure among TRPA1, TRPV1, and TRPV4 could clarify the mechanisms of pore size fluctuation.

Experimental procedures

Chemicals

AITC and carvacrol were obtained from Wako Pure Chemical Industries. Capsaicin, crotamiton dimethylamine solution (DMA), menthol, methylamine solution (MMA), NMDG, and 2-aminoethoxydiphenylborane (2-APB) were obtained from Sigma-Aldrich. GSK was obtained from Tocris Bioscience. Tetramethylammonium hydroxide pentahydrate (TetMA) was obtained from Tokyo Chemical Industry. Stock solutions were prepared in ethanol for AITC, capsaicin, carvacrol, crotamiton, and menthol and in dimethyl sulfoxide (Wako) for GSK and 2-APB.

Cell culture

HEK293T cells were maintained at 37 °C in 5% CO_2 in Dulbecco's modified Eagle's medium (Wako) containing 10% fetal bovine serum (FBS, BioWest), 50 units mL^{-1} penicillin/50 μg mL^{-1} streptomycin (Life Technologies) and 2 mM L-glutamine (GlutaMAX™, Life Technologies). NHEK (Adult, KURABO) were maintained at 37 °C in 5% CO_2 in Humedia-KG2 (KURABO).

Transient transfection of HEK293T cells

Transient transfection of HEK293 cells was achieved with Lipofectamine® Transfection Reagent (Life Technologies), PLUS™ Reagent (Life Technologies), and Opti-MEM® I Reduced Serum Medium (Life Technologies), following the manufacturer's protocol. Plasmid DNAs (m*TRPA1*/pcDNA5-FRT, m*TRPM8*/pcDNA5-FRT, m*TRPV1*/pcDNA3.1, m*TRPV2*/pcDNA3 m*TRPV3*/pcDNA3, m*TRPV4*/pcDNA3, and h*TRPV4*/pcDNA3) were transfected with pGreen Lantern 1 into HEK293T cells and transfected cells were used for patch-clamp experiments 14–48 h after transfection.

Electrophysiology

HEK293T cells expressing each TRP channel and NHEK were used for whole-cell recordings and those expressing mTRPV4 were used for single-channel recordings as well with standard patch pipettes (3–8 MΩ resistance) made with borosilicate glass capillaries (King Precision Glass). The extracellular solution for whole-cell recording was a

standard bath solution containing 140 mM NaCl, 5 mM KCl, 2 mM $CaCl_2$, 2 mM $MgCl_2$, 10 mM HEPES, and 10 mM D-glucose at pH 7.4, adjusted with NaOH. A calcium-free bath solution was prepared by omitting 2 mM $CaCl_2$ from the standard bath solution and adding 5 mM EGTA. The extracellular solution for single-channel recording and the intracellular solutions for both whole-cell and inside-out patch-clamp configurations contained 140 mM KCl, 5 mM EGTA, 2 mM $MgCl_2$, and 10 mM HEPES at pH 7.4, adjusted with KOH. The whole-cell voltage-clamp recordings were performed with the membrane potential clamped at −60 mV. Voltage-ramp pulses from −100 to +100 mV within 500 ms were applied every 5 s. Inside-out membrane patches were used for single-channel recordings where the membrane potential was clamped at −60 mV. Before membrane excision, cells were perfused with the standard bath solution that was then exchanged for the KCl-based solution. Sodium-substituted solutions were prepared by exchanging sodium for methylamines, the tetraammonium ions, and NMDG, which were listed in "Chemicals." Data were sampled at 10 kHz and filtered at 5 kHz for whole-cell recording and at 2 kHz for single-channel recording (Axopatch 200B Amplifier, Molecular Devices). Data were analyzed using pCLAMP 10.4 Software (Molecular Devices).

Behavior test

Male C57BL/6N mice (9- to 11-week-old) were kept in a controlled environment (12 h light/dark cycle, 22–25 °C, 50–60% humidity) with food and water provided ad libitum, with 2–4 animals per cage. All experiments were performed during the light cycle. The day before the experiment, the hair on the backs of the mice was clipped. Prior to scratch recording (1.5 h), the mice were put into a cage for acclimation. Crotamiton oil or saline (30 μL) was applied to the bare skin of the mice 0.5 h before recording. After subcutaneous injection of GSK (10 nmol/50 μL/site), scratching behaviors were recorded with a camera (NEX-5K, SONY).

Statistics

Data were expressed as means ± SEM. No data points were excluded. All statistical analyses were conducted in at least three different experiments. Statistical analyses were performed with the two-tailed Welch's *t* test to compare two groups and with the ANOVA followed by Tukey's test for multiple comparisons. We used an ORIGIN 8.1 software for data fitting. $P < 0.05$ was considered to be significant.

Acknowledgements This work was supported by the Japanese Ministry of Education, Culture, Sports, Science and Technology Grants 16K21691 (to H. K.), 15H02501 (to M. T.), and 15H05928 (to M. T.).

Author contributions H. K. and Y. Y. designed and performed the experiments. H. K., Y. Y., and M. T wrote the manuscript.

Compliance with ethical standards

Conflict of interest The authors declare that they have no conflicts of interest with the contents of this article.

Funding This work was supported by the Japanese Ministry of Education, Culture, Sports, Science and Technology Grants 16K21691 (to H. K.), 15H02501 (to M. T.), and 15H05928 (to M. T.).

References

1. Akiyama T, Ivanov M, Nagamine M, Davoodi A, Carstens MI, Ikoma A, Cevikbas F, Kempkes C, Buddenkotte J, Steinhoff M, Carstens E (2016) Involvement of TRPV4 in serotonin-evoked scratching. J Invest Dermatol 136:154–160. doi:10.1038/JID.2015.388
2. Burckhardt W, Rymarowicz R (1946) Erfahrungen mit dem neuen Antiscabiosum Eurax (Geigy). Schweiz Med Wochenschr 76:1213
3. Cao E, Liao M, Cheng Y, Julius D (2013) TRPV1 structures in distinct conformations reveal activation mechanisms. Nature 504:113–118. doi:10.1038/nature12823
4. Caterina MJ, Schumacher MA, Tominaga M, Rosen TA, Levine JD, Julius D (1997) The capsaicin receptor: a heat-activated ion channel in the pain pathway. Nature 389:816–824. doi:10.1038/39807
5. Caterina MJ, Rosen TA, Tominaga M, Brake AJ, Julius D (1999) A capsaicin-receptor homologue with a high threshold for noxious heat. Nature 398:436–441. doi:10.1038/18906
6. Chen J, Kim D, Bianchi BR, Cavanaugh EJ, Faltynek CR, Kym PR, Reilly RM (2009) Pore dilation occurs in TRPA1 but not in TRPM8 channels. Mol Pain 5:3. doi:10.1186/1744-8069-5-3
7. Chen Y, Fang Q, Wang Z, Zhang JY, MacLeod AS, Hall RP, Liedtke WB (2016) Transient receptor potential vanilloid 4 ion channel functions as a pruriceptor in epidermal keratinocytes to evoke histaminergic itch. J Biol Chem 291:10252–10262. doi:10.1074/jbc.M116.716464
8. Christensen AP, Akyuz N, Corey DP (2016) The outer pore and selectivity filter of TRPA1. PLoS One 11:e0166167. doi:10.1371/journal.pone.0166167
9. Chung MK, Lee H, Mizuno A, Suzuki M, Caterina MJ (2004) TRPV3 and TRPV4 mediate warmth-evoked currents in primary mouse keratinocytes. J Biol Chem 279:21569–21575. doi:10.1074/jbc.M401872200
10. Chung MK, Guler AD, Caterina MJ (2005) Biphasic currents evoked by chemical or thermal activation of the heat-gated ion channel, TRPV3. J Biol Chem 280:15928–15941. doi:10.1074/jbc.M500596200
11. Chung MK, Guler AD, Caterina MJ (2008) TRPV1 shows dynamic ionic selectivity during agonist stimulation. Nat Neurosci 11:555–564. doi:10.1038/nn.2102
12. Couperus M (1949) The use of N-ethyl-o-crotonotoluidide in the treatment of scabies and various pruritic dermatoses. J Invest Dermatol 13:35–42
13. Domenjoz R (1946) Ueber ein neues Antiscabiosum (Crotonsäure-N-aethyl-o-toluidid). Schweiz Med Wochenschr 76:1210–1213

14. Garcia-Elias A, Mrkonjic S, Pardo-Pastor C, Inada H, Hellmich UA, Rubio-Moscardo F, Plata C, Gaudet R, Vicente R, Valverde MA (2013) Phosphatidylinositol-4,5-biphosphate-dependent rearrangement of TRPV4 cytosolic tails enables channel activation by physiological stimuli. Proc Natl Acad Sci U S A 110:9553–9558. doi:10.1073/pnas.1220231110
15. Grant AD, Cottrell GS, Amadesi S, Trevisani M, Nicoletti P, Materazzi S, Altier C, Cenac N, Zamponi GW, Bautista-Cruz F, Lopez CB, Joseph EK, Levine JD, Liedtke W, Vanner S, Vergnolle N, Geppetti P, Bunnett NW (2007) Protease-activated receptor 2 sensitizes the transient receptor potential vanilloid 4 ion channel to cause mechanical hyperalgesia in mice. J Physiol 578:715–733. doi:10.1113/jphysiol.2006.121111
16. Guler AD, Lee H, Iida T, Shimizu I, Tominaga M, Caterina M (2002) Heat-evoked activation of the ion channel, TRPV4. J Neurosci 22:6408–6414 20026679
17. Han SK, Mancino V, Simon MI (2006) Phospholipase Cbeta 3 mediates the scratching response activated by the histamine H1 receptor on C-fiber nociceptive neurons. Neuron 52:691–703. doi:10.1016/j.neuron.2006.09.036
18. Huynh KW, Cohen MR, Jiang J, Samanta A, Lodowski DT, Zhou ZH, Moiseenkova-Bell VY (2016) Structure of the full-length TRPV2 channel by cryo-EM. Nat Commun 7:11130. doi:10.1038/ncomms11130
19. Ikoma A, Steinhoff M, Stander S, Yosipovitch G, Schmelz M (2006) The neurobiology of itch. Nat Rev Neurosci 7:535–547. doi:10.1038/nrn1950
20. Imamachi N, Park GH, Lee H, Anderson DJ, Simon MI, Basbaum AI, Han SK (2009) TRPV1-expressing primary afferents generate behavioral responses to pruritogens via multiple mechanisms. Proc Natl Acad Sci U S A 106:11330–11335. doi:10.1073/pnas.0905605106
21. Jordt SE, Bautista DM, Chuang HH, McKemy DD, Zygmunt PM, Hogestatt ED, Meng ID, Julius D (2004) Mustard oils and cannabinoids excite sensory nerve fibres through the TRP channel ANKTM1. Nature 427:260–265. doi:10.1038/nature02282
22. Karashima Y, Prenen J, Talavera K, Janssens A, Voets T, Nilius B (2010) Agonist-induced changes in Ca(2+) permeation through the nociceptor cation channel TRPA1. Biophys J 98:773–783. doi:10.1016/j.bpj.2009.11.007
23. Khakh BS, Bao XR, Labarca C, Lester HA (1999) Neuronal P2X transmitter-gated cation channels change their ion selectivity in seconds. Nat Neurosci 2:322–330. doi:10.1038/7233
24. Kim BM, Lee SH, Shim WS, Oh U (2004) Histamine-induced Ca(2+) influx via the PLA(2)/lipoxygenase/TRPV1 pathway in rat sensory neurons. Neurosci Lett 361:159–162. doi:10.1016/j.neulet.2004.01.019
25. Kim S, Barry DM, Liu XY, Yin S, Munanairi A, Meng QT, Cheng W, Mo P, Wan L, Liu SB, Ratnayake K, Zhao ZQ, Gautam N, Zheng J, Karunarathne WK, Chen ZF (2016) Facilitation of TRPV4 by TRPV1 is required for itch transmission in some sensory neuron populations. Sci Signal 9:ra71. doi:10.1126/scisignal.aaf1047
26. Kittaka H, Tominaga M (2017) The molecular and cellular mechanisms of itch and the involvement of TRP channels in the peripheral sensory nervous system and skin. Allergol Int 66:22–30. doi:10.1016/j.alit.2016.10.003
27. Lenggenhager R (1947) Erfahrungen mit neuen Antiskabiosa. Praxis 36:465
28. Li M, Toombes GE, Silberberg SD, Swartz KJ (2015) Physical basis of apparent pore dilation of ATP-activated P2X receptor channels. Nat Neurosci 18:1577–1583. doi:10.1038/nn.4120
29. Liao M, Cao E, Julius D, Cheng Y (2013) Structure of the TRPV1 ion channel determined by electron cryo-microscopy. Nature 504:107–112. doi:10.1038/nature12822
30. Liedtke W, Choe Y, Marti-Renom MA, Bell AM, Denis CS, Sali A, Hudspeth AJ, Friedman JM, Heller S (2000) Vanilloid receptor-related osmotically activated channel (VR-OAC), a candidate vertebrate osmoreceptor. Cell 103:525–535
31. Lin Z, Chen Q, Lee M, Cao X, Zhang J, Ma D, Chen L, Hu X, Wang H, Wang X, Zhang P, Liu X, Guan L, Tang Y, Yang H, Tu P, Bu D, Zhu X, Wang K, Li R, Yang Y (2012) Exome sequencing reveals mutations in TRPV3 as a cause of Olmsted syndrome. Am J Hum Genet 90:558–564. doi:10.1016/j.ajhg.2012.02.006
32. McKemy DD, Neuhausser WM, Julius D (2002) Identification of a cold receptor reveals a general role for TRP channels in thermosensation. Nature 416:52–58. doi:10.1038/nature719
33. Montell C, Rubin GM (1989) Molecular characterization of the Drosophila trp locus: a putative integral membrane protein required for phototransduction. Neuron 2:1313–1323
34. Morita T, McClain SP, Batia LM, Pellegrino M, Wilson SR, Kienzler MA, Lyman K, Olsen AS, Wong JF, Stucky CL, Brem RB, Bautista DM (2015) HTR7 mediates serotonergic acute and chronic itch. Neuron 87:124–138. doi:10.1016/j.neuron.2015.05.044
35. Munns CH, Chung MK, Sanchez YE, Amzel LM, Caterina MJ (2015) Role of the outer pore domain in transient receptor potential vanilloid 1 dynamic permeability to large cations. J Biol Chem 290:5707–5724. doi:10.1074/jbc.M114.597435
36. Muraki K, Iwata Y, Katanosaka Y, Ito T, Ohya S, Shigekawa M, Imaizumi Y (2003) TRPV2 is a component of osmotically sensitive cation channels in murine aortic myocytes. Circ Res 93:829–838. doi:10.1161/01.RES.0000097263.10220.0C
37. Naziroglu M, Ozgul C, Celik O, Cig B, Sozbir E (2011) Aminoethoxydiphenyl borate and flufenamic acid inhibit Ca2+ influx through TRPM2 channels in rat dorsal root ganglion neurons activated by ADP-ribose and rotenone. J Membr Biol 241:69–75. doi:10.1007/s00232-011-9363-9
38. Paulsen CE, Armache JP, Gao Y, Cheng Y, Julius D (2015) Structure of the TRPA1 ion channel suggests regulatory mechanisms. Nature 520:511–517. doi:10.1038/nature14367
39. Peier AM, Moqrich A, Hergarden AC, Reeve AJ, Andersson DA, Story GM, Earley TJ, Dragoni I, McIntyre P, Bevan S, Patapoutian A (2002) A TRP channel that senses cold stimuli and menthol. Cell 108:705–715
40. Peier AM, Reeve AJ, Andersson DA, Moqrich A, Earley TJ, Hergarden AC, Story GM, Colley S, Hogenesch JB, McIntyre P, Bevan S, Patapoutian A (2002) A heat-sensitive TRP channel expressed in keratinocytes. Science 296:2046–2049. doi:10.1126/science.1073140
41. Rothman S (1941) Physiology of itching. Physiol Rev 21:357–381
42. Shim WS, Tak MH, Lee MH, Kim M, Kim M, Koo JY, Lee CH, Kim M, Oh U (2007) TRPV1 mediates histamine-induced itching via the activation of phospholipase A2 and 12-lipoxygenase. J Neurosci 27:2331–2337. doi:10.1523/JNEUROSCI.4643-06.2007
43. Smith GD, Gunthorpe MJ, Kelsell RE, Hayes PD, Reilly P, Facer P, Wright JE, Jerman JC, Walhin JP, Ooi L, Egerton J, Charles KJ, Smart D, Randall AD, Anand P, Davis JB (2002) TRPV3 is a temperature-sensitive vanilloid receptor-like protein. Nature 418:186–190. doi:10.1038/nature00894
44. Story GM, Peier AM, Reeve AJ, Eid SR, Mosbacher J, Hricik TR, Earley TJ, Hergarden AC, Andersson DA, Hwang SW, McIntyre P, Jegla T, Bevan S, Patapoutian A (2003) ANKTM1, a TRP-like channel expressed in nociceptive neurons, is activated by cold temperatures. Cell 112:819–829
45. Strotmann R, Harteneck C, Nunnenmacher K, Schultz G, Plant TD (2000) OTRPC4, a nonselective cation channel that confers sensitivity to extracellular osmolarity. Nat Cell Biol 2:695–702. doi:10.1038/35036318

46. Surprenant A, Rassendren F, Kawashima E, North RA, Buell G (1996) The cytolytic P2Z receptor for extracellular ATP identified as a P2X receptor (P2X7). Science 272:735–738
47. Thorneloe KS, Sulpizio AC, Lin Z, Figueroa DJ, Clouse AK, McCafferty GP, Chendrimada TP, Lashinger ES, Gordon E, Evans L, Misajet BA, Demarini DJ, Nation JH, Casillas LN, Marquis RW, Votta BJ, Sheardown SA, Xu X, Brooks DP, Laping NJ, Westfall TD (2008) N-((1S)-1-{[4-((2S)-2-{[(2,4-dichlorophenyl)sulfonyl]amino}-3-hydroxypropanoyl)-1 -piperazinyl]carbonyl}-3-methylbutyl)-1-benzothiophene-2-carboxamide (GSK1016790A), a novel and potent transient receptor potential vanilloid 4 channel agonist induces urinary bladder contraction and hyperactivity: part I. J Pharmacol Exp Ther 326:432–442. doi:10.1124/jpet.108.139295
48. Togashi K, Hara Y, Tominaga T, Higashi T, Konishi Y, Mori Y, Tominaga M (2006) TRPM2 activation by cyclic ADP-ribose at body temperature is involved in insulin secretion. EMBO J 25:1804–1815. doi:10.1038/sj.emboj.7601083
49. Tominaga M, Caterina MJ, Malmberg AB, Rosen TA, Gilbert H, Skinner K, Raumann BE, Basbaum AI, Julius D (1998) The cloned capsaicin receptor integrates multiple pain-producing stimuli. Neuron 21:531–543
50. Venkatachalam K, Montell C (2007) TRP channels. Annu Rev Biochem 76:387–417. doi:10.1146/annurev.biochem.75.103004.142819
51. Virginio C, MacKenzie A, Rassendren FA, North RA, Surprenant A (1999) Pore dilation of neuronal P2X receptor channels. Nat Neurosci 2:315–321. doi:10.1038/7225
52. Voets T, Prenen J, Vriens J, Watanabe H, Janssens A, Wissenbach U, Bodding M, Droogmans G, Nilius B (2002) Molecular determinants of permeation through the cation channel TRPV4. J Biol Chem 277:33704–33710. doi:10.1074/jbc.M204828200
53. Vriens J, Owsianik G, Hofmann T, Philipp SE, Stab J, Chen X, Benoit M, Xue F, Janssens A, Kerselaers S, Oberwinkler J, Vennekens R, Gudermann T, Nilius B, Voets T (2011) TRPM3 is a nociceptor channel involved in the detection of noxious heat. Neuron 70:482–494. doi:10.1016/j.neuron.2011.02.051
54. Watanabe H, Davis JB, Smart D, Jerman JC, Smith GD, Hayes P, Vriens J, Cairns W, Wissenbach U, Prenen J, Flockerzi V, Droogmans G, Benham CD, Nilius B (2002) Activation of TRPV4 channels (hVRL-2/mTRP12) by phorbol derivatives. J Biol Chem 277:13569–13577. doi:10.1074/jbc.M200062200
55. Watanabe H, Vriens J, Suh SH, Benham CD, Droogmans G, Nilius B (2002) Heat-evoked activation of TRPV4 channels in a HEK293 cell expression system and in native mouse aorta endothelial cells. J Biol Chem 277:47044–47051. doi:10.1074/jbc.M208277200
56. Watanabe H, Vriens J, Prenen J, Droogmans G, Voets T, Nilius B (2003) Anandamide and arachidonic acid use epoxyeicosatrienoic acids to activate TRPV4 channels. Nature 424:434–438. doi:10.1038/nature01807
57. Wilson SR, Gerhold KA, Bifolck-Fisher A, Liu Q, Patel KN, Dong X, Bautista DM (2011) TRPA1 is required for histamine-independent, mas-related G protein-coupled receptor-mediated itch. Nat Neurosci 14:595–602. doi:10.1038/nn.2789
58. Wilson SR, The L, Batia LM, Beattie K, Katibah GE, McClain SP, Pellegrino M, Estandian DM, Bautista DM (2013) The epithelial cell-derived atopic dermatitis cytokine TSLP activates neurons to induce itch. Cell 155:285–295. doi:10.1016/j.cell.2013.08.057
59. Xu H, Ramsey IS, Kotecha SA, Moran MM, Chong JA, Lawson D, Ge P, Lilly J, Silos-Santiago I, Xie Y, DiStefano PS, Curtis R, Clapham DE (2002) TRPV3 is a calcium-permeable temperature-sensitive cation channel. Nature 418:181–186. doi:10.1038/nature00882
60. Zubcevic L, Herzik MA Jr, Chung BC, Liu Z, Lander GC, Lee SY (2016) Cryo-electron microscopy structure of the TRPV2 ion channel. Nat Struct Mol Biol 23:180–186. doi:10.1038/nsmb.3159